HR-MAS NMR Spectroscopy in the Characterization of Human Tissues: Application to Healthy Gastric Mucosa

LUISA SCHENETTI,[1] ADELE MUCCI,[1] FRANCESCA PARENTI,[1] RITA CAGNOLI,[1] VALERIA RIGHI,[1, 3] M. RAFFAELLA TOSI,[2] VITALIANO TUGNOLI[3]

[1] *Dipartimento di Chimica, Università di Modena e Reggio Emilia, Via G. Campi, 183, I-41100 Modena, Italy*
[2] *ITOI-CNR, Sez. di Bologna, c/o IOR, Via di Barbiano 1/10, 40136 Bologna, Italy*
[3] *Dipartimento di Biochimica G. Moruzzi, Università di Bologna, Via Belmeloro 8/2, 40126 Bologna, Italy*

ABSTRACT: The HR-MAS is an ideal technique for the investigation of intact tissue specimens (10–50 mg) and permits the obtainment of spectra with a resolution comparable to that observed in solution in a time that does not exceed a half of an hour for a routine analysis. The potentialities of HR-MAS NMR spectroscopy in the identification of the metabolites characterizing the healthy gastric mucosa are here presented. The direct inspection of the 1D ^{1}H NMR spectra enables only few metabolites to be confidently assigned, and the use of selected 2D experiments strongly amplify the analytical effectiveness of the technique. Concepts Magn Reson Part A 28A: 430–443, 2006

KEY WORDS: ex vivo HR-MAS; metabolites; gastric mucosa; 2D NMR spectroscopy

INTRODUCTION

NMR is a powerful tool for the structure determination of biomolecules and natural compounds, for the study of tissue extracts or intact tissues, and for obtaining detailed three-dimensional maps of the human body and organs. In the field of biomedicine, the two areas of NMR are represented by magnetic resonance imaging (MRI) and by the multibranched magnetic

Received 3 April 2006; revised 28 July 2006; accepted 1 August 2006

Correspondence to: Luisa Schenetti; E-mail address: schene@unimo.it

Concepts in Magnetic Resonance Part A, Vol. 28A(6) 430–443 (2006)

Published online in Wiley InterScience (www.interscience.wiley.com). DOI 10.1002/cmr.a.20068

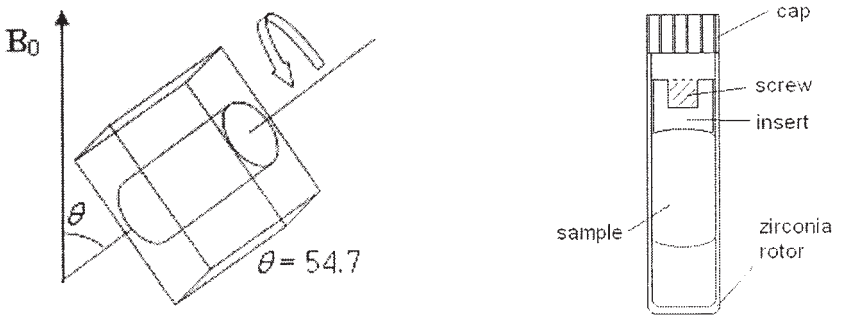

Figure 1 Schematic representation of HR-MAS probe (left); HR-MAS rotor (right).

resonance spectroscopy (MRS), where MRS is the acronym used in place of NMR. MRI uses the strong signals from water protons to provide detailed anatomical maps and has proven to be an indispensable tool for researchers and clinicians, but its specificity in defining the pathology is limited to only some diseases. In vivo MRS provides the spectra of living tissues, directly correlated to their chemical composition but, due to the low mobility of the majority of tissue components, which sensibly broaden the signal line widths, and to the signals overlapping, only few metabolites can be distinguished and assigned unambiguously. The in vivo MRS (*1–3*) is considered a radiological tool able to help the imaging methods in the evaluation of several human pathologies, including cancer. Nevertheless, in vivo MRS can be used when the molecular markers of tissues are well established by means of a detailed biochemical picture, which can be derived from the spectroscopic analysis of in vitro extracts (aqueous or lipidic) of tissues or cells and from ex vivo biopsy samples using high-resolution magic angle spinning (HR-MAS) NMR technique.

HR-MAS NMR can be considered a hybrid technique between solid-state NMR and classical solution state NMR. It uses, similar to solid-state NMR, the magic angle spinning (MAS) (*4*), but it retains the classical solution NMR experiments. Similar to solution NMR, HR-MAS NMR involves direct polarization transfer and not cross-polarization transfer (CP-MAS) (*5*) between ^{1}H and heteronuclei (^{13}C or ^{15}N), thus distinguishing it from CP-MAS experiments on true solids.

HR-MAS uses dedicated probeheads capable of studying the samples in rapid rotation (3 ÷ 15 kHz) around an axis 54.7° ("magic angle") tilted with respect to that of the static magnetic field (B_0) (Fig. 1). These probeheads drastically reduce contributions from dipolar couplings, chemical shift anisotropy, and susceptibility distortions, providing high-resolution spectra from semisolid samples, such as tissues. The quality of the obtained spectra is comparable to that obtained from aqueous extracts, and the acquisition techniques used are those employed in high-resolution NMR in solution. The advantage is that of carrying out the measurements on intact tissue specimens, without any pretreatment enabling the extraction step to be omitted, and aqueous and lipid fractions to be detected simultaneously, enhancing the possibility of identifying biochemical markers with diagnostic and prognostic value. After the first applications of HR-MAS NMR on human tissue specimens (*6*, *7*), some articles on ex vivo HR-MAS spectroscopic studies on different organ tissues have appeared (*8–10*) .

Here we present the application of HR-MAS NMR to the ex vivo characterization of healthy gastric mucosa tissues. These findings will form a rational basis for in vivo MRS in the evaluation of neoplasms of human gastric mucosa cancer, which is a leading cause of cancer-related deaths in many parts of the world (*11*, *12*).

SAMPLE SELECTION AND TREATMENT

The samples chosen should be representative of the gastric mucosa, and, in particular, the biopsies should be obtained on healthy tissues that do not present visible macroscopic alterations. The tissues are to be considered healthy only when the histologic examination confirms the macroscopic finding, mainly when these studies are undertaken for the first time. The original samples are to be put rapidly in liquid nitrogen and stored at −85°C until NMR analyses. The samples can be preserved up to 3 months without observing changes in the spectra, and the measurements should be taken within this period. Immediately before NMR analysis, the tissue sample is cut to have suitable dimensions and flushed with D_2O to eliminate residual blood (thus reducing the iron content, with the aim to improve the homogeneity, and in turn the water suppression) and to add deuterium as

nucleus for the lock system. The specimens are then transferred into the MAS zirconia rotors (4 mm OD) that are available in different capacities (12, 50, 90 μL), and are chosen in relation to the sample amount. A Teflon perforated insert is used to restrict the volume, to eliminate bubbles, and to improve the homogeneity of the sample. The insert is closed by a screw, then the rotor by a cap—the star shape of which provides the driving for the rotor (see Fig. 1). The rotor is then placed in the stator and the sample spun at 4000 Hz. The rotation rate is selected to have the spinning sidebands out of the region of interest (~10 ppm). The temperature of the sample is maintained at 278 K to limit sample degradation. Sample and instrument preparation takes about 20 min.

HR-MAS NMR MEASUREMENTS

One-Dimensional NMR Spectra

The NMR experiments in obtaining HR-MAS spectra of tissues are the same as those used in solution. A generally employed basic set of experiments is formed by:

1. The 1D ^{1}H NMR experiment with suppression of the residual HDO/H_2O generates a spectrum containing signals from metabolites, macromolecules, and lipids. It is necessary to suppress water signal because its high intensity can obscure the resonances of the other components. Among several approaches that can be adopted (*13*), the presaturation one is that preferred by us. It consists in the irradiation of the HDO/H_2O signal with a weak radiofrequency field B_1 (50 Hz) for some seconds prior to the acquisition of the ^{1}H spectrum. This method is more selective than others, but it is not recommended when peaks from protons involved in chemical exchange processes with water are studied, because their signals are reduced or lost.
2. The water-suppressed spin-echo experiment (Carr-Purcell-Meiboom-Gill, CPMG) (*14*) acting as a T_2 filter cuts off signals from macromolecules and lipids, leaving only signals from small metabolites. The experiment employs the pulse sequence:

$$[\mathbf{d_1\text{-}90^\circ\text{-}(\tau\text{-}180^\circ\text{-}\tau)_n\text{-}AQ}]$$

where d_1 is the relaxation delay, τ the echo time, and AQ the acquisition time. The 90° pulse creates a transverse magnetization that decays during the spin-echo period $(\tau\text{-}180^\circ\text{-}\tau)_n$. Macromolecules having short T_2 [T_2 can be estimated by the half-height line width $l_{w1/2}$ by the equation $l_{w1/2}=1/(\pi T_2)$] should be completely relaxed and filtered out. The echo time $2n\tau$ can be varied in relation to the T_2 of the macromolecules. The water suppression irradiation is used during d_1 and is conventionally set to 1.5 ms.

3. The gradient-based stimulated-echo pulse sequence (with bipolar-gradient pulse pairs and longitudinal-eddy current delay, LED) (*15*) generates a spectrum in which signals coming from slowly diffusing molecules are retained at expenses of those from low molecular weight metabolites, which are, in turn, reduced. The experiment employs the following pulse sequence:

$$[\mathbf{d_1\text{-}90\text{-}g_1\text{-}\delta\text{-}180\text{-}g_2\text{-}\delta\text{-}90\text{-}g_3\text{-}\Delta\text{-}90\text{-}g_1\text{-}\delta\text{-}180\text{-}g_2\text{-}\delta\text{-}90\text{-}g_4\text{-}d_{21}\text{-}90\text{-}AQ}]$$

where $g_2 = -g_1$, the diffusion time d_{20} = 90-δ-180-δ-90-Δ and d_{21} is the eddy-current time. The correct selection of d_{20} and the gradient strength permits to filter out signals from fast moving small molecules and to retain only macromolecules.

These last two experiments exploit the different relaxation and diffusion properties of small metabolites with respect to macromolecules and lipids. The accurate choice of the spin-spin relaxation delay $2n\tau$ and of parameters influencing diffusion (gradient-field pulse duration δ, gradient strength, and diffusion time Δ) enables two complementary sets of signals, corresponding to narrow and broad components, to be isolated. The acquisition of a diagnostic set of 1D HR-MAS spectra requires about 30 min, but the correct and complete attribution of the whole resonances is based on 2D techniques, which require much more time.

Two-Dimensional NMR Spectra

2D NMR spectra can be a valuable aid in elucidating complex NMR spectra, permitting identification of unknown compounds mainly by analyzing their spin-spin correlations through chemical bonds. Among the plethora of 2D experiments found in the literature, the most effective, and thus most commonly employed, for the identifications of metabolites in mixtures are COrrelation SpectroscopY (COSY) (*16*), TOtal Cor-

relation SpectroscopY (TOCSY) (*17*, *18*), and Heteronuclear Single Quantum Coherence (HSQC) (*19*) or Heteronuclear Multiple Quantum Coherence (HMQC) (*20*) experiments.

1. COSY experiments, based on the transfer of spin information between coupled spins, afford spectra as 2D plots in which signals corresponding to the 1D spectrum are on the diagonal, whereas off-diagonal peaks, called cross-peaks, are found between pairs of coupled spins. These correlations are usually due to connections through two and three bonds, but long-range connectivities can sometimes be observed.
2. TOCSY experiments enable all the components of a spin system to be detected (at least in principle). The core of these experiments is a spin-lock time, which allows transfer of information from one spin to another belonging to the same coupling network, even if these spins are separated by many bonds. The mixing time must be held long enough (from 60 to 140 ms) to complete the transfer process to all the spins. The TOCSY spectra permit the identification of $^{1}H,^{1}H$ connectivities up to five or six bonds.
3. Inverse-detection experiments HMQC and HSQC enable pairs of protons and carbons directly bonded to be found. These are basically heteronuclear COSY experiments that rely on the acquisition of the more receptive nucleus (i.e., the proton), whereas the chemical shift of the heteronucleus is found in the second dimension. The knowledge of the carbon chemical shift associated to the proton one represents a key step in the identification of a metabolite.

To acquire a complete set of good-quality 2D spectra, 15–20 hours of acquisition are required.

EXPERIMENTAL DETAILS

Proton HR-MAS spectra were recorded with a Bruker Avance400 spectrometer equipped with a $^{1}H/^{13}C$ HR-MAS probe (operating at 400.13 and 100.61 MHz, respectively) and with a Bruker Cooling Unit (BCU) for temperature control. Samples were spun at 4000 Hz, and three different types of 1D proton spectra were acquired using sequences implemented in the Bruker software: (i) a standard sequence with 1.5 s water presaturation during relaxation delay, 8 kHz spectral width, 32k data points, 32–64 scans, (ii) a water-suppressed spin-echo CPMG sequence with 1.5 s water presaturation during relaxation delay, 1 ms echo time (τ) and 360 ms total spin-spin relaxation delay ($2n\tau$), 8 kHz spectral width, 32k data points, 256 scans, and (iii) a sequence for diffusion measurements based on stimulated echo and bipolar-gradient pulses with big delta 200 ms, eddy current delay T_e 5 ms, little delta 2*2 ms, sine-shaped gradient with 32 G/cm followed by a 200 μs delay for gradient recovery, 8 kHz spectral width, 8k data points, and 256 scans. Two-dimensional COSY spectra were acquired using a standard pulse sequence and 0.5 s water presaturation during relaxation delay, 8 kHz spectral width, 4k data points, 32 scans per increment, and 256 increments. Two-dimensional TOCSY spectra were acquired using a standard pulse sequence and 1 s water presaturation during relaxation delay, 100 ms mixing (spin-lock) time, 4 kHz spectral width, 4k data points, 32 scans per increment, and 128 increments. Two-dimensional HSQC spectra were acquired using a standard pulse sequence echo-antiecho phase sensitive and 0.5 s relaxation delay, 1.725 ms evolution time, 4 kHz spectral width in f_2, 4k data points, 128 scans per increment, 17 kHz spectral width in f_1, and 256 increments.

It is not necessary to add a reference standard for the chemical shift scale, such as TSP (trimethylsilylpropansulfonate), but our suggestion is to use a well-known resonance as internal standard, such as H-1 of α-glucose (Glc) (a doublet at 5.24 ppm, J = 3.8 Hz) or the methyl of alanine (Ala) or lactate (Lac) (doublets at 1.48 ppm, J = 7.2 Hz, and 1.33 ppm, J = 6.9 Hz, respectively). Attention should be paid when using the signal of HDO to calibrate the chemical shift scale, for it is highly temperature dependent.

TEMPERATURE EFFECTS

All samples were studied under temperature control conditions, at 278 K. This was necessary to slow down tissue degradation processes, which are found to be more evident at room temperature. Two sets of representative 1D proton spectra obtained at 300 and 278 K at different times (0 and 18–21 h) from two samples of normal gastric mucosa are displayed in Fig. 2. They were all acquired using a water-presaturation sequence with composite pulse and are informative of small and large metabolites present in the tissue. The two spectra at t = 0 (a and c) are similar, except for a different intensity of the signal at 3.72 ppm due to polyethylene glycol (PEG), used as an excipient in pharmaceutical preparations, and for a slightly better spectral resolution in the case of c). After almost 1 day, an increase in the signals of small metabolites, more evident at the higher work temper-

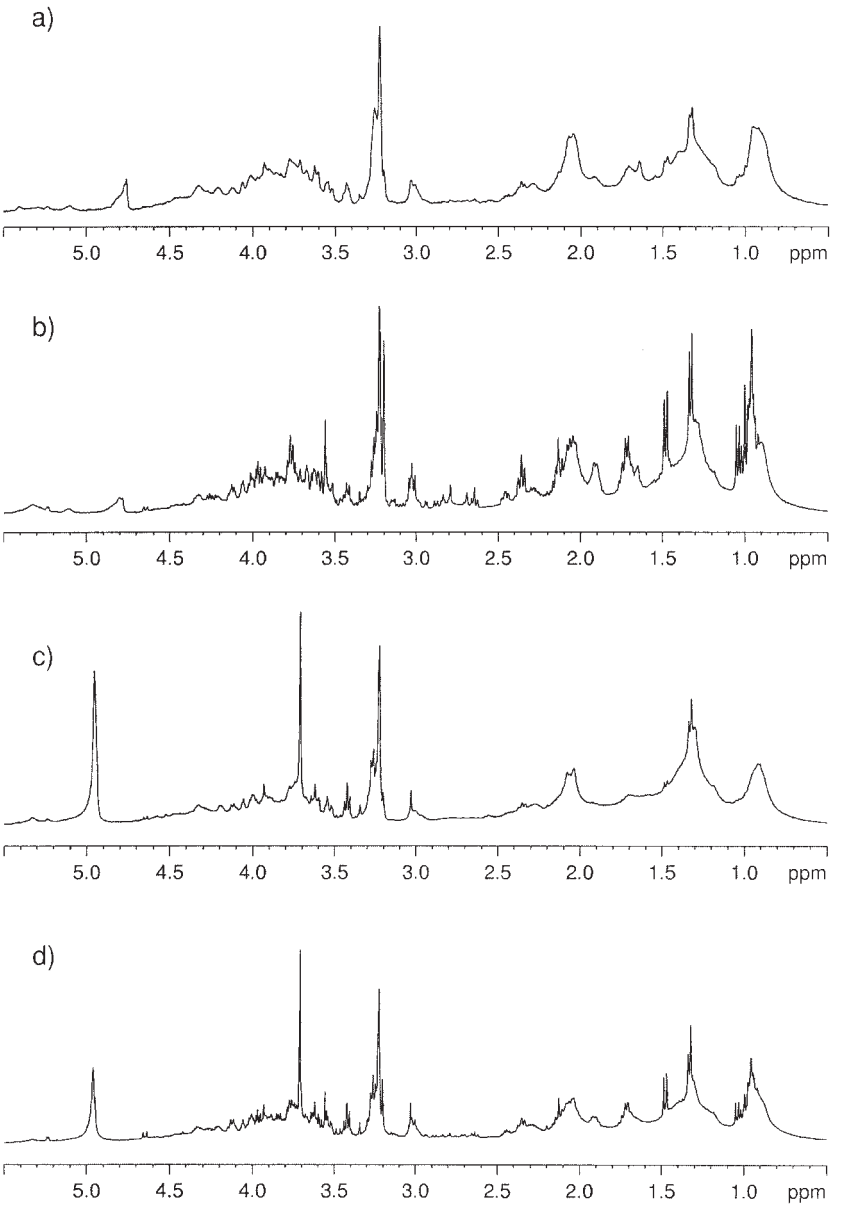

Figure 2 1D water-presaturated ^{1}H NMR spectra of healthy gastric mucosa: (a) sample 1 at 300 K, t = 0 h; (b) sample 1 at 300 K, t = 21 h; (c) sample 2 at 278 K, t = 0 h; (d) sample 2 at 278 K, t = 18 h.

ature (see b versus d), can be observed. These spectral changes are attributable to the increased mobility of some metabolites and to the partial disruption of subcellular structures, probably due to temperature and spinning. Degradation symptoms only slightly affect the samples in the first hour of analysis and, in the view of future applications of HR-MAS with diagnostic purposes, they do not have to be overemphasized. Nevertheless, these findings prompted us to work at 278 K, especially to safely acquire 2D spectra, which are more time-consuming than the 1D ones.

METABOLITES ANALYSIS

A pool of 10 biopsies from healthy gastric mucosa were studied. Typically, three 1D experiments were recorded for each sample (Fig. 3). The water-presaturated 1D spectrum (see Fig. 3a) displays the contribution of the resonances deriving from small metabolites with long spin-spin relaxation times T_2, hence narrow bandwidth, that can be readily distinguished from that of macromolecules and lipids with short

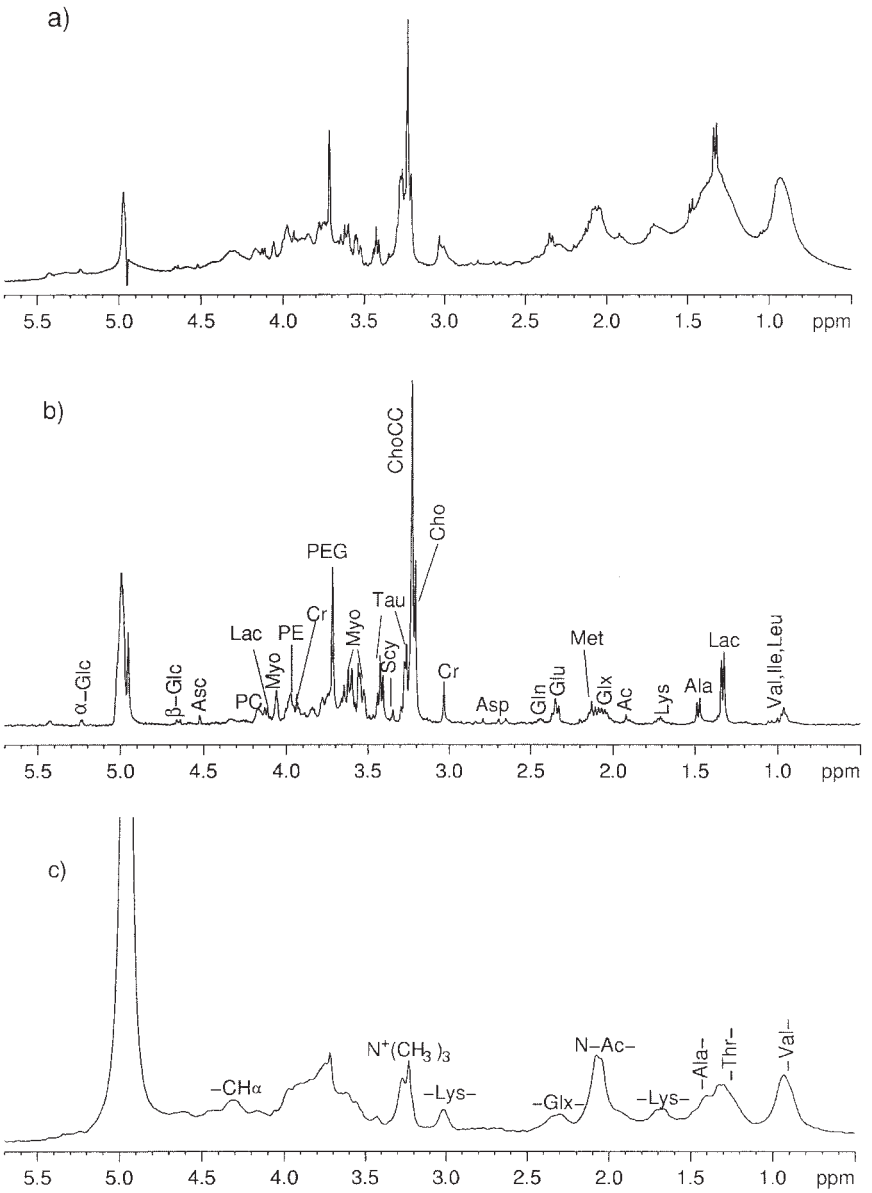

Figure 3 1D proton NMR spectra of healthy gastric mucosa obtained with (a) water-presaturation pulse sequence with composite pulse; (b) CPMG sequence with total spin-echo time $2n\tau = 360$ ms; (c) diffusion-edited spectrum obtained with $\Delta = 200$ ms, $\delta = 4$ ms and gradient strength of 32 G/cm. The metabolites are identified according to Table 1.

(but not so short to be NMR invisible) T_2, hence large bandwidth. The CPMG spin-echo sequence eliminates the contribution of the broad resonances and retains only narrow signals from small molecules (see Fig. 3b). The diffusion-edited spectrum permits to observe components with low diffusion rates and large line width, mainly deriving from lipids, in the present case phospholipids, and mobile peptidic residues (see Fig. 3c).

It is apparent, especially to a trained eye, that some metabolites [e.g., doublets at 1.33 and 1.48 ppm for Lac and Ala, respectively; triplets at 2.36 and 3.42 ppm for glutamate (Glu) and taurine (Tau), respectively; singlets at 3.04, 3.20, 3.22, 3.56 ppm for creatine (Cr), choline (Cho), glycerophosphorylcholine + phosphorylcholine (GPC + PC) and glycine (Gly), respectively; multiplets at 4.06, 3.63 and 3.53 for myo-inositol (Myo)] can be readily assigned by direct inspection of the 1D ^{1}H NMR spectra, mainly the spin-echo one, and by comparison with literature data, but a complete and unambiguous assignment requires the acquisition of selected 2D experiments.

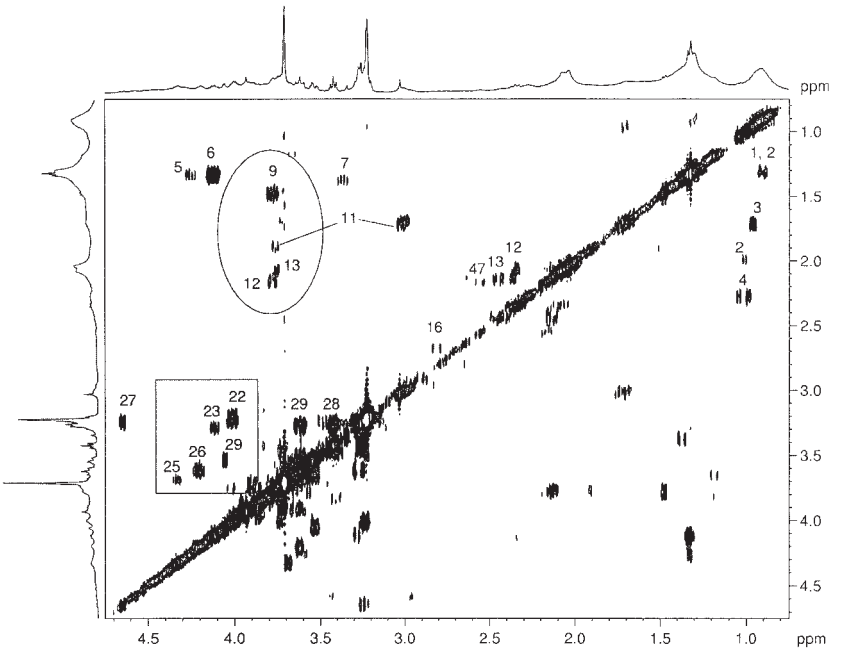

Figure 4 COSY NMR spectrum of healthy gastric mucosa. The identified metabolites are labeled according to Table 1.

We found that COSY, TOCSY, and HSQC spectra are the most effective in this respect (whereas *J*-resolved experiments are less suitable). They all are highly informative for the identification of hidden resonances. In particular, the HSQC experiment makes possible a more reliable assignment of signals, by comparison of ^{1}H and ^{13}C data with those of the literature, and the distinction among signals from different molecules having similar proton chemical shifts but diverse ^{13}C signals. The COSY and TOCSY spectra (Figs. 4 and 5) allow us to detect a pool of metabolites, especially osmolites and free amino acids. The COSY spectra are particularly useful for the distinction of Lac and threonine (Thr), whose doublets at 1.33 ppm overlap, and for the detection of α-hydrogens of several amino acids (circled in Fig. 4). They also allow us to distinguish GPC from PC, whose $N^{+}(CH_3)_3$ signals are usually unresolved, and to detect phosphorylethanolamine (PE), whose signals are found in a crowded region and often hidden under those of other metabolites (squared in Fig. 4). In all the examined samples except one, two unknown coupled signals (a triplet at 1.37 and a quartet at 3.37 ppm) were detected in the COSY spectra. The assignment of these signals is discussed elsewhere.

Some metabolites, such as lysine (Lys) and arginine (Arg) (circled in Fig. 5), Myo, and β-Glc are better differentiated in TOCSY spectra. More interestingly, some signals due to α-CH of bonded amino acids (mainly Ala and Thr) are detected in the region of the 2D spectrum close to the correlations of Lac and Thr (squared in Fig. 5), and only low correlations are found for bonded valine (Val). These findings confirm the presence of mobile peptidic residues that is apparent from the examination of the diffusion-edited spectra (see Fig. 3c). The amino acids involved in the peptidic chains are mainly those carrying aliphatic or substituted aliphatic chains, being the aromatic region of the proton spectra almost empty. Some weak correlations attributable to the protons belonging to fatty acid chains are sometimes detected through both 2D experiments. Nevertheless, those due to glycerol protons in triglycerides, at 5.26, 4.30, and 4.10 ppm, are evident only in one COSY spectrum (*21*).

Further progresses toward the identification of metabolites can be done exploiting the ^{13}C chemical shift dispersion in the second dimension of HSQC experiments. A region of interest is usually that corresponding to the $N^{+}(CH_3)_3$ of choline-containing compounds (ChoCC), Tau, Arg, Myo, and PE, which contribute all to the 3.2 ppm signal in the proton spectra. These molecules can readily be distinguished in HSQC spectra (Fig. 6) due to the large differences in their ^{13}C chemical shifts (circled in Fig. 6) and also to their multiplicity (CH_3 vs. CH_2), if edited sequences are employed (*22*). Some problems are encountered in the interpretation of the region between

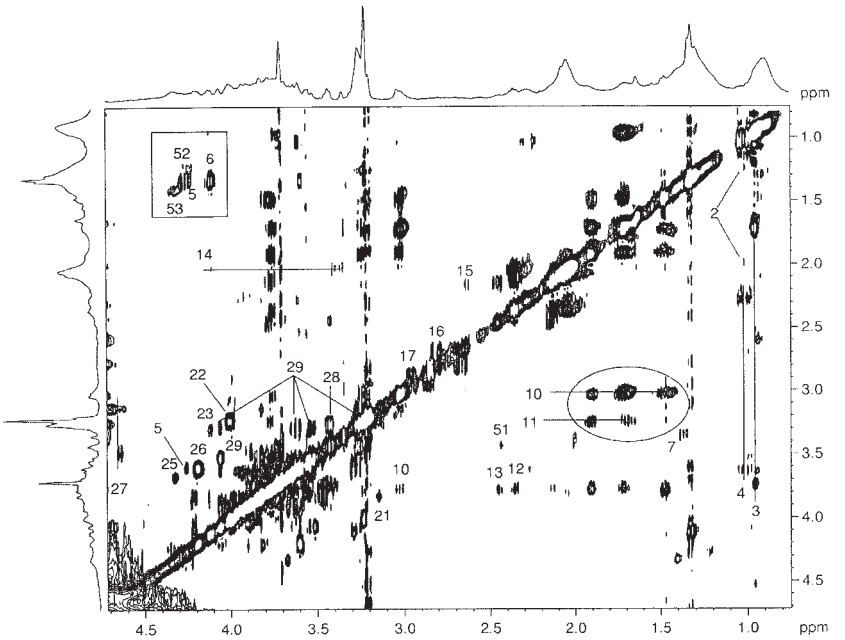

Figure 5 TOCSY NMR spectrum of healthy gastric mucosa. The identified metabolites are labeled according to Table 1.

3.6 and 4.0 ppm, for the presence of overlapped correlations around 62 ppm, presumably due to glycerols and CH_2OH of Glc. All sample spectra show also a more or less strong resonance at 3.72 (s) ppm due to PEG, as confirmed by the ^{13}C resonance at 70.3 ppm, used as an excipient in pharmaceuticals.

The ^{13}C chemical shifts dispersion is also useful for the assignment of the signals of aliphatic amino acids [isoleucine (Ile), Val, leucine (Leu)] (Fig. 7).

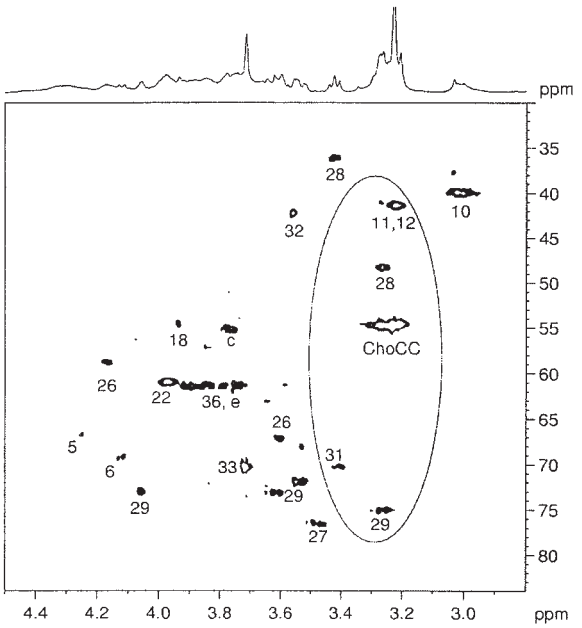

Figure 6 Partial $^{1}H,^{13}C$-HSQC spectrum of healthy gastric mucosa. The identified metabolites are labeled according to Table 1.

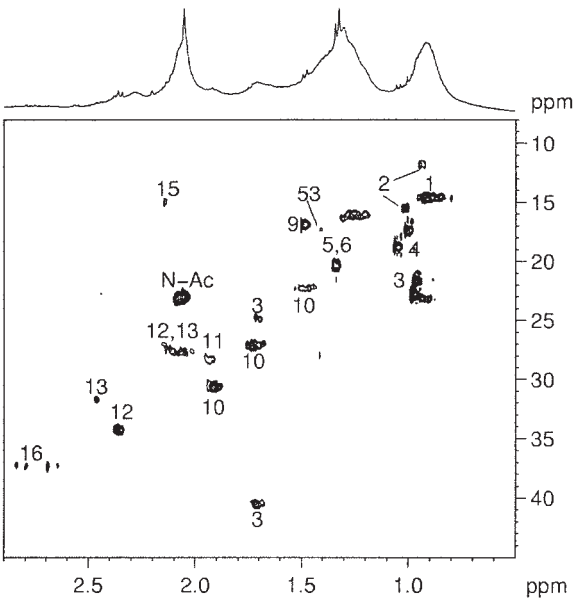

Figure 7 Partial $^{1}H,^{13}C$-HSQC spectrum of healthy gastric mucosa. The identified metabolites are labeled according to Table 1.

The observed peaks seem to be principally related to the narrow components appearing in the CPMG spectrum (Fig. 3b), with the exception of signals due to *N*-acetyl (N-Ac) groups (probably arising from sialic acid present in glycoproteins or from oligopeptide components), which are instead evidenced in the diffusion-edited spectrum (see Fig. 3c).

The accurate inspection of COSY, TOCSY, and HSQC spectra allows us to find signals not directly attributable to metabolites. Besides signals from PEG already mentioned, the assignment of other two unknown signals (a triplet at 1.37 and a quartet at 3.37 ppm), detected in the COSY and TOCSY spectra, was rather intriguing. The chemical shift of their directly bonded carbons in the HSQC spectrum is 9.2 and 50.7 ppm, respectively. These H,C chemical shifts are compatible with those of a molecule containing an ethyl group bonded to a positively charged nitrogen and were assigned to the ethyl group of lidocaine chlorohydrate, which is used as anesthetic prior to endoscopy. The comparison of the CPMG spectrum of healthy stomach with that of an authentic sample allows us to assign to lidocaine chlorohydrate also another unidentified singlet, at 2.20 ppm (carbon at 17.8 ppm), and a multiplet, at 7.28 ÷ 7.16 ppm, due to the methyls bonded to phenyl ring and to the aromatic protons, respectively. Only the signal coming from the CH_2 bridging the N^+ and to the amidic carbonyl, expected as a singlet at 4.33 ppm (carbon at 53.7 ppm), was not distinguished, probably because it is obscured by the OCH_2 signal of GPC. Eventually, a correlation detected in COSY and TOCSY spectra, between protons at 5.08 and 2.03 ppm, can be attributed to another excipient (i.e., cetylpyridinium) present together with PEG in the lidocaine solution. The signal at 5.08 ppm can be directly observed in the water-presaturated and in the diffusion-edited spectra, whereas, unlike lidocaine, it is absent in the CPMG spectra. The application of the whole experiments to samples of normal human gastric mucosa permitted the complete and unambiguous identification of the metabolic pattern typical of this tissue (Table 1).

Further remarks on the relative contents of some metabolites in healthy gastric mucosa can be done. Regarding the ChoCC, the ^{1}H NMR spectra evidence that the PC content is similar or higher than that of GPC, whereas Cho is present in smaller amount with respect to its phosphorylated analogues in all the examined samples. The mean ChoCC/Cho ratio, derived from the integrated areas of $N^+(CH_3)_3$ in CPMG experiments, is 5 ± 2 (standard deviation). The ratio ChoCC/Cr (derived from the integrated areas of the $N^+(CH_3)_3$ signal of ChoCC and the NCH_3 signal of Cr) and the ratio ChoCC/Tau (derived from the integrated areas of the $N^+(CH_3)_3$ signal of ChoCC and the NCH_2 signal of tau) are found around 16 ± 4 and 7 ± 1, respectively.

At the present, the use of in vivo MR spectroscopy in the study of gastric mucosa is not feasible because of the difficulties coping with gastric wall movements. However, the findings reported here should provide the rational bases for the interpretation of the in vivo MR spectra and its use for diagnostic purposes, in the view of future in vivo methodology developments. Some peculiarities of ex vivo and in vivo MR spectra are to be considered before attempting a direct comparison. The in vivo ^{1}H MR spectra of human tissues are acquired using spin-echo sequences (PRESS or STEAM) at two different echo times (TE 38 and 144 ms). The signal-to-noise ratio is higher and the spectra display more signals when the shorter TE is used. The spectra obtained in vivo at the longer TE display fewer resonances due to the more marked reduction of the signals of macromolecules and lipids with respect to those of small metabolites. Whatever the experiment employed, the in vivo spectra always show signals broader than those present in the ex vivo ones. To compare the two types of experiments, it is necessary to apply to ex vivo spectra a line broadening (5–20 Hz) function, generating signal bandwidths similar to those found in in vivo ones. The in vivo spectra obtained at TE 38 and 144 ms should be compared with the standard 1D and the CPMG spectra, respectively. Eventually, MRS users should be aware that the in vivo signals at 3.03 ppm receives contributions not only from Cr but also from bonded Lys, whereas that generally attributed to ChoCC, at 3.23 ppm, receives contributions also from Tau, Arg, Myo, Glc, and PE.

CONCLUSIONS

We have shown that HR-MAS is an ideal method for the analysis of intact tissue specimens, allowing spectra to be obtained with a resolution comparable to that observed in solution. It requires only small amounts of tissue (10–50 mg); routine analysis does not exceed a half of an hour; and it enables small and large metabolites to be detected simultaneously.

The application of ^{1}H and ^{13}C HR-MAS NMR allowed us to fully characterize the molecular composition of healthy gastric mucosa. The use of suitable 1D and 2D experiments allowed us to identify the NMR signals from more than 50 species. Among them only a few can be confidently assigned by direct inspection of the 1D ^{1}H NMR spectra, whereas 2D COSY, TOCSY, and HSQC strongly amplify the

Table 1 List of ^{1}H and ^{13}C Chemical Shift (δ, ppm) of Metabolites and Exogenous Molecules Found in HR-MAS Spectra of Healthy Gastric Mucosa[a,b]

Entry	Metabolite	δ ^{1}H	δ ^{13}C	
1	Fatty acids	0.89	14.13–14.17	CH_3
		1.31	29.4–32.2	$(CH_2)_n$
		1.59–1.60	25.2	$CH_2CC{=}O$
		2.02	27.8	$CH_2C{=}$
		2.24	34.2	$CH_2C{=}O$
		2.78	26.2	$={=}CCH_2C{=}$
		5.30–5.32	130.2; 128.4	$CH{=}CH$
2	Isoleucine	0.94 (t)	11.7	δ-CH_3
		1.02 (d)	15.5	γ-CH_3
		1.29, 1.48	25.1	γ-CH_2
		1.97		β-CH
		3.69		α-CH
3	Leucine	0.95 (d)	21.5	δ-CH_3
		0.97 (d)	22.8	δ-CH_3
		1.70	24.8	γ-CH
		1.72	40.4	β-CH_2
		3.74		α-CH
4	Valine	0.99 (d)	17.3	γ-CH_3
		1.04 (d)	18.7	γ-CH_3
		2.25		β-CH
		3.61	d	α-CH
5	Threonine	1.33 (d)	20.3	γ-CH_3
		4.26	66.6	β-CH
		3.60	61.2	α-CH
6	Lactate	1.33 (d)	20.3	CH_3
		4.11	69.1	CH
7	Lidocaine chlorohydrate	1.37 (t)	9.2	CH_3
		3.37 (q)	50.6	CH_2
		2.20 (s)	17.8	2,6-CH_3
8	β-Alanine	2.56	32.1	CH_2
		3.18	40.0	CH_2
9	Alanine	1.48 (d)	16.8	β-CH_3
		3.78	51.1	α-CH
10	Lysine	3.02 (t)	39.9	ε-CH_2
		1.71	27.1	δ-CH_2
		1.48	22.6	γ-CH_2
		1.91	30.6	β-CH_2
		3.79	c	α-CH
11	Arginine	3.23	41.3	δ-CH_2
		1.69		γ-CH_2
		1.92	28.1	β-CH_2
		3.78	c	α-CH
12	Glutamate	2.36 (t)	34.0	γ-CH_2
		2.06, 2.14	27.9	β-CH_2
		3.77	c	α-CH
13	Glutamine	2.44 (td)	31.5	γ-CH_2
		2.14	27.2	β-CH_2
		3.78	c	α-CH
14	Proline	3.43, 3.34		δ-CH_2
		2.01		γ-CH_2
		2.34, 2.07		β-CH_2
		4.12		α-CH

(*continued*)

Table 1 ***(Continued)***

Entry	Metabolite	δ ^{1}H	δ ^{13}C	
15	Methionine	2.13 (s)	14.9	SCH_3
		2.62		γ-CH_2
		2.16		β-CH_2
		3.87		α-CH
16	Aspartic acid	2.68, 2.82	37.2	β-CH_2
		3.90		α-CH
17	Asparagine	2.85, 2.96	26.3	β-CH_2
		4.01		α-CH
18	Creatine	3.04 (s)	37.5	NCH_3
		3.92 (s)	54.5	CH_2
19	Tyrosine	3.06, 3.20		β-CH_2
		3.93	56.7	α-CH
		6.89	116.5	H*ortho*
		7.23	131.5	H*meta*
20	Phenylalanine	3.11, 3.28		β-CH_2
		3.99		α-CH
		7.34	130.1	H*ortho*
		7.43	129.6	H*meta*
		7.37		H*para*
21	Ethanolamine	3.15 (t)		CH_2
		3.82 (t)		CH_2
22	Phosphorylethanolamine	3.23	41.1	CH_2
		4.00	61.1	CH_2
23	Glycerophosphorylethanolamine	3.30		CH_2
		4.10		CH_2
24	Free choline	3.20	54.6	$N(CH_3)_3$
		3.53	68.2	NCH_2
		4.08	56.5	OCH_2
25	Glycerophosphorylcholine	3.22	54.7	$N(CH_3)_3$
		3.68		NCH_2
		4.33		OCH_2
26	Phosphorylcholine	3.22	54.7	$N(CH_3)_3$
		3.61	67.3	NCH_2
		4.22	59.0	OCH_2
27	β-Glucose	4.67 (d)	96.6	1-CH
		3.26	74.8	2-CH
		3.49	76.8	3-CH
		3.40	69.9	4-CH
		3.47	76.8	5-CH
		e	e	6-CH_2
28	Taurine	3.26 (t)	48.1	SCH_2
		3.42 (t)	35.9	NCH_2
29	Myoinositol	3.53 (dd)	71.8	1,3-CH
		4.06 (t)	72.9	2-CH
		3.63 (t)	73.1	4,6-CH
		3.29(t)	75.0	5-CH
30	Scyllo-inositol	3.35 (s)	73.9	CH
31	α-Glucose	5.24 (d)		1-CH
		3.54	72.5	2-CH
		3.73	73.8	3-CH
		3.42	70.7	4-CH
		e	e	6-CH_2
32	Glycine	3.56	42.3	CH_2
33	PEG	3.72	69.9	
34	Glycerol (in lipids)	4.10, 4.30		1,3-CH_2
		5.26		2-CH

(*continued*)

Table 1 *(Continued)*

Entry	Metabolite	δ ^{1}H	δ ^{13}C	
35	Glycerol	3.56, 3.65	63.3	1-CH_2
		3.81	72.7	2-CH
36	Bonded glycerols	3.95–3.70	61.3	1,3-CH_2
37	UDP	5.92		1-CHrib
		4.35		2-CHrib
		5.90 (d)		5-CHur
		7.89 (d)		6-CHur
38	Uracil	5.80 (d)		5-CHur
		7.54 (d)		6-CHur
39	UMP	5.98		1-CHrib
		4.37		2-CHrib
		5.97 (d)		5-CHur
		8.11 (d)		6-CHur
40	Formiate	8.48		
41	Adenosine	8.36 (s)		
		8.23 (s)		
42	Acetate	1.92	24.8	$CH_3C{=}O$
43	Hypotaurine	2.65 (t)	38.7	SCH_2
		3.35 (t)	41.2	NCH_2
44	Tryptophane	7.73		
		7.19		
		7.29		
		7.52		
45	αGlc-1-X	5.40	100.2	
		3.61		
46	Glutathione	4.57	56.2	α-CH-Cys
		2.96	26.3	β-CH_2-Cys
		3.80		α-CH-Glu
		2.16		β-CH_2-Glu
		2.55		γ-CH_2-Glu
		3.77	44.0	CH_2-Gly
		8.57		NH-Cys
		8.36		NH-Gly
47	OH-butyrate	1.18		CH_3
		4.14		
48	Histidine	7.78 (s)		2-CH
		7.05 (s)		4-CH
49	Ascorbate	4.52 (d)		4-CH
		4.01		5-CH
50	Unknown	1.63	23.5	
51	Unknown	2.44		
		3.44		
52	Bonded Thr	1.22	16.2	γ-CH_3
		4.24		β-CH
		4.31		α-CH
53	Bonded Ala	1.41	17.1	β-CH_3
		4.32		α-CH
54	Bonded Val	0.93	23.0	γ-CH_3
		2.08		β-CH
		4.11		α-CH
55	Cetylpyridinium	5.08		NCH_2
		2.03		β-CH_2

[a] ^{1}H chemical shift are referred to alanine doublet at 1.48 ppm.
[b] ^{13}C chemical shift are referred to alanine at 16.8 ppm.
[c] Cα probably contributes to the 3.77, 55.1 ppm cross-peak.
[d] Cα probably contributes to the 3.61, 61.1 ppm cross-peak.
[e] Contribute to the broad correlation between CH_2 protons in the region 3.9 ÷ 3.6 ppm and carbons around 62 ppm in HSQC spectra.

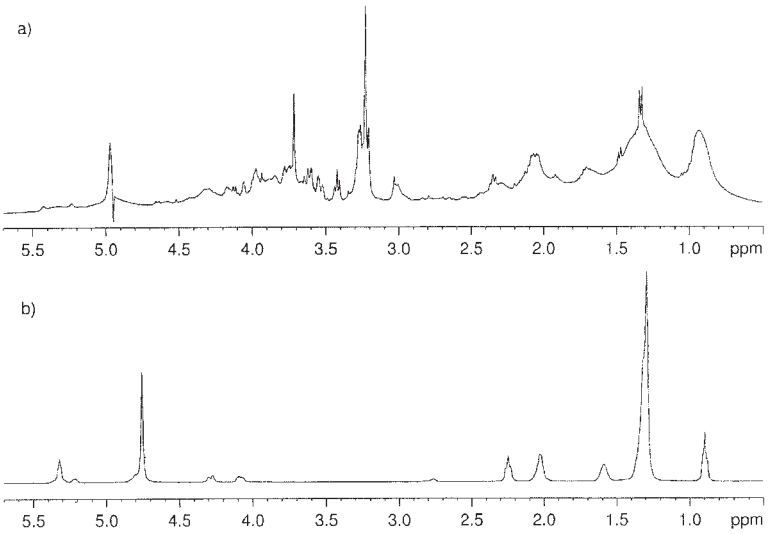

Figure 8 1D ^{1}H NMR spectra of healthy gastric mucosa (a) and adenocarcinoma (b).

analytical effectiveness of the technique. The effectiveness of ex vivo ^{1}H HR-MAS NMR in giving an accurate description of the metabolic pattern of the examined tissues enhances notably if we consider that it can provide useful information for the interpretation of in vivo MRS measurements. The two types of spectra can be compared directly when the differences due to echo times and line width are taken into account. HR-MAS actually gives the molecular bases for the interpretation of the in vivo spectra.

Moreover, this method is well suited to provide complementary information to histopathology. What probably still lacks for the use of HR-MAS with diagnostic purposes are larger evaluation studies aimed at the statistical validation of the ^{1}H profiles for healthy and unhealthy tissues. The first tests performed in our laboratories show that the NMR profile of gastric neoplastic mucosa is completely different from that of the healthy one (Fig. 8), making us foresee a strong diagnostic impact of in vivo, when implemented, and ex vivo NMR in this field.

The adenocarcinoma proton spectrum is characterized by predominant signals due to triglycerides, as confirmed by the presence of signals due to glycerol (5.26, 4.30, and 4.10 ppm) and to long fatty acid chains (saturated and unsaturated). Otherwise, the healthy mucosa spectrum indicates that triglycerides are present in low amounts.

Eventually, we have here reported that signals from exogenous molecules, such as lidocaine, PEG, and cetylpyridinium, have been detected in almost all the examined samples. These findings make us envisage another application of HR-MAS NMR, in conjunction with in vivo MRS—the detection of drugs or the metabolic changes induced by them.

ACKNOWLEDGMENTS

The Fondazione Cassa di Risparmio di Modena is acknowledged for the financial support given for the acquisition of the Bruker Avance400 Spectrometer. The Centro Interdipartimentale Grandi Strumenti of the University of Modena and Reggio Emilia is acknowledged for the use of it.

REFERENCES

1. Kwoch L, Smith JK, Castillo M, Ewend MG, Cush S, Hensing T, et al. 2002. Clinical applications of proton MR spectroscopy in oncology. Technol Cancer Res Treat 1:17–28.
2. Tosi R, Tugnoli V, editors. 2005. Nuclear magnetic resonance spectroscopy in the study of neoplastic tissue. New York: Nova Science Publishers, Inc.
3. Gillies RJ, Morse DL. 2005. In vivo magnetic resonance spectroscopy in cancer. Annu Rev Biomed Eng 7:287–326.
4. Andrew ER, Bradbury A, Eades RG. 1959. Removal of dipolar broadening of nuclear magnetic resonance spectra of solids by specimen rotation. Nature 183:1802–1803.
5. Stejskal EO, Schaefer J, Waugh JS. 1977. Magic-angle spinning and polarization transfer in proton-enhanced NMR. J Magn Reson 28:105–112.
6. Cheng LL, Ma MJ, Becerra L, Ptak T, Tracey I, Lack-

ner A, Gonzalez RG. 1997. Quantitative neuropathology by high resolution magic angle spinning proton magnetic resonance spectroscopy. Proc Natl Acad Sci U S A 94:6408–6413.
7. Tomlins AM, Foxall PJD, Lindon JC, Nicholson JK, Lynch MJ, Spraul M, Everett JR. 1998. High resolution magic angle spinning ^{1}H NMR analysis of intact prostatic hyperplastic and tumor tissues. Anal Comm 35: 113–115.
8. Tugnoli V, Schenetti L, Mucci A, Nocetti L, Toraci C, Mavilla L, et al. 2005. A comparison between in vivo and ex vivo HR-MAS ^{1}H MR spectra of a pediatric poster fossa lesion. Int J Mol Med 16:301–307.
9. Sitter B, Bathen T, Hagen B, Arentz C, Skjeldestad FE, Gribbestad IS. 2004. Cervical cancer tissue characterized by high-resolution magic angle spinning MR spectroscopy. MAGMA 16:174–181.
10. Martinez-Granados B, Monleon D, Martinez-Bisbal MC, Rodrigo JM, del Olmo J, Lluch P, et al. 2006. Metabolite identification in human liver needle biopsies by high-resolution magic angle spinning 1H NMR spectroscopy. NMR Biomed 19:90–100.
11. Murray CJ, Lopez AD. 1997. Alternative projections of mortality and disability by cause 1990-2020:Global Burden of Disease Study. Lancet 349: 1498–1504.
12. Rudy DR, Zdon MJ. 2000. Update on colorectal cancer. Am Fam Phys 61:1759–1770, 1773–1774.
13. Price WS. 1999. Water signal suppression in NMR spectroscopy. In: Webb GA, editor. Annual reports on NMR spectroscopy. London: Academic Press. p 289–354.
14. Meiboom S, Gill D. 1958. Modified spin-echo method for measuring nuclear relaxation time. Rev Sci Instrum 29:688–691.
15. Wu DH, Chen A, Johnson CS Jr. 1995. An improved diffusion-ordered spectroscopy experiment incorporating bipolar gradient pulses. Magn Reson A 115:260–264.
16. Aue WP, Bartholdi E, Ernst RR. 1976. Two-dimensional spectroscopy. Application to nuclear magnetic resonance. J Chem Phys 64:2229–2246.
17. Bax A, Davis DG. 1985. MLEV-17-based two-dimensional homonuclear magnetization transfer spectroscopy. J Magn Reson 65:355–360.
18. Braunschweiler L, Ernst RR. 1983. Coherence transfer by isotropic mixing: application to proton correlation spectroscopy. J Magn Reson 53:521–528.
19. Bodenhausen G, Ruben DJ. 1980. Natural abundance nitrogen-15 NMR by enhanced heteronuclear spectroscopy. Chem Phys Lett 69:185–189.
20. Müller L. 1979. Sensitivity enhanced detection of weak nuclei using heteronuclear multiple quantum coherence. J Am Chem Soc 101:4481–4484.
21. Tugnoli V, Mucci A, Schenetti L, Calabrese C, Di Febo G, Rossi MC, Tosi MR. 2004. Molecular characterization of human gastric mucosa by HR-MAS magnetic resonance spectroscopy. Int J Mol Med 14:1065–1071.
22. Willker W, Leibfritz D, Kerssebaum R, Bermel W. 1993. Gradient selection in inverse heteronuclear correlation spectroscopy. Magn Reson Chem 31:287–292.

BIOGRAPHY

Luisa Schenetti received her master's degree in chemistry under the mentorship of Prof. F. Taddei at the University of Modena in 1970. She is full professor in organic chemistry at the University of Modena e Reggio Emilia. Her main research activities include application of the HR-MAS technique in the study of healthy and neoplastic human tissues and NMR characterization of natural and synthetic polymers.